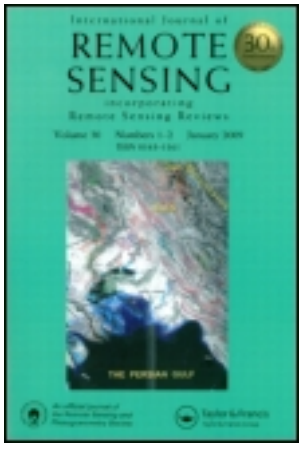

International Journal of Remote Sensing

Publication details, including instructions for authors and subscription information:
http://www.tandfonline.com/loi/tres20

Ground-, satellite- and simulation-based analysis of a strong dust event over Abastumani, Georgia, during May 2009

P. Kokkalis [a], R. E. Mamouri [a], M. Todua [b], G. G. Didebulidze [b], A. Papayannis [a], V. Amiridis [c], S. Basart [d], C. Pérez [e] & J. M. Baldasano [d f]

[a] Laser Remote Sensing Laboratory, Department of Physics, National Technical University of Athens, Athens, Greece

[b] Georgian National Astrophysical Observatory, Ilia State University, Tbilisi, Georgia

[c] Institute for Space Applications and Remote Sensing, National Observatory of Athens, Athens, Greece

[d] Earth Sciences Division, Barcelona Supercomputing Centre, Barcelona, Spain

[e] The Earth Institute at Columbia University, NASA Goddard Institute for Space Studies and The International Research Institute for Climate and Society, New York, NY, USA

[f] Environmental Modelling Laboratory, Project Engineering Department, Universitat Politècnica de Catalunya, Barcelona, Spain

Available online: 06 Feb 2012

To cite this article: P. Kokkalis, R. E. Mamouri, M. Todua, G. G. Didebulidze, A. Papayannis, V. Amiridis, S. Basart, C. Pérez & J. M. Baldasano (2012): Ground-, satellite- and simulation-based analysis of a strong dust event over Abastumani, Georgia, during May 2009, International Journal of Remote Sensing, 33:16, 4886-4901

To link to this article: http://dx.doi.org/10.1080/01431161.2011.644593

International Journal of Remote Sensing
Vol. 33, No. 16, 20 August 2012, 4886–4901

Taylor & Francis
Taylor & Francis Group

Ground-, satellite- and simulation-based analysis of a strong dust event over Abastumani, Georgia, during May 2009

P. KOKKALIS†, R. E. MAMOURI†, M. TODUA‡, G. G. DIDEBULIDZE‡, A. PAPAYANNIS*†, V. AMIRIDIS§, S. BASART¶, C. PÉREZ| and J. M. BALDASANO¶,††

†Laser Remote Sensing Laboratory, Department of Physics, National Technical University of Athens, Athens, Greece
‡Georgian National Astrophysical Observatory, Ilia State University, Tbilisi, Georgia
§Institute for Space Applications and Remote Sensing, National Observatory of Athens, Athens, Greece
¶Earth Sciences Division, Barcelona Supercomputing Centre, Barcelona, Spain
|The Earth Institute at Columbia University, NASA Goddard Institute for Space Studies and The International Research Institute for Climate and Society, New York, NY, USA
††Environmental Modelling Laboratory, Project Engineering Department, Universitat Politècnica de Catalunya, Barcelona, Spain

(*Received 1 July 2010; in final form 10 October 2011*)

A strong dust event over Abastumani, Georgia, during May 2009 was studied using light detection and ranging (lidar), satellite and sun photometric measurements. High aerosol optical depth (AOD) values (0.45–0.57) at 500 nm were measured over the closest Aerosol Robotic Network (AERONET) site (Erdemli, Turkey), whereas over Georgia, the AOD measured by the Moderate Resolution Imaging Spectroradiometer (MODIS) was about 0.9 at 550 nm. The AERONET data analysis showed a mean aerosol effective radius of about 2.5 μm, whereas the mean value of the Ångström exponent (α) (wavelength pair 440/870 nm) was smaller than 1, indicating the dominance of large aerosols. The aerosol lidar over Abastumani showed the existence of a strong particle load from the near ground up to a height of 3.5 km. The BSC-DREAM8b forecast model showed that the dust aerosols travelled from the Saharan and the Arabic deserts to the studied area, even reaching southern Russia, covering a total distance of about 5500 km, in the height region from about 2 to 11.5 km.

1. Introduction

Tropospheric aerosols arise from both natural (windborne dust, sea spray, forest fires and volcanic eruptions) and anthropogenic (combustion of fossil fuels, car traffic and biomass burning activities) sources. According to the latest report of the Intergovernmental Panel on Climate Change (IPCC) (Forster *et al.* 2007), the climatic role of dust aerosols is now better quantified than in the past; thus, a total direct aerosol radiative forcing, combined across all aerosol types, can now be given as -0.5 ± 0.4 W m^{-2}, with a medium-low level of scientific understanding. The shortwave radiative forcing of dust aerosols can be either positive or negative, depending

*Corresponding author. Email: apdlidar@central.ntua.gr

International Journal of Remote Sensing
ISSN 0143-1161 print/ISSN 1366-5901 online © 2012 Taylor & Francis
http://www.tandf.co.uk/journals
http://dx.doi.org/10.1080/01431161.2011.644593

on the vertical distribution of dust, the underlying cloud cover and the surface albedo. On the other hand, the longwave radiative forcing is always positive (Tegen *et al.* 1996, Ramanathan *et al.* 2007). However, the overall uncertainties in the radiative forcing effect of dust (anthropogenic and natural) still remain very high. These uncertainties can only be reduced by better quantifying the vertical and horizontal distribution of dust in the globe. Light detection and ranging (lidar) aerosol measurements of the vertical distribution of the optical properties of dust can contribute to such quantification.

Mineral dust is an important component of the atmospheric aerosol loading. According to Kinne *et al.* (2006), mineral dust accounts for about 75% of the global aerosol mass load and 25% of the global aerosol optical depth (AOD). The African continent, especially its northern part (Sahara desert), the Saudi Arabian regions and the Asian continent (eastern areas) are the main sources of dust around the globe (Marticorena *et al.* 1997, Prospero *et al.* 2002, Engelstaedter and Washington 2007, Liu *et al.* 2008a,b).

Georgia is mostly affected by dust particles coming from closely located desert areas over Iraq, Syria and the Arabian Peninsula. However, distant desert areas, such as the Saharan region, also have effects on air quality over the Mediterranean region (Rodriguez *et al.* 2001, Prospero *et al.* 2002, Papayannis *et al.* 2005, Pérez *et al.* 2006a, Escudero *et al.* 2007a,b, Querol *et al.* 2009a,b). However, no references in the international literature are yet available about such events in the Georgian territory; thus, this study is the first ever performed in that area. In this article, we first introduce the instrumentation and methods followed to study a strong dust event over Georgia. Then, ground-based measurements are presented and discussed along with dust model estimations and satellite observations. Finally we present our conclusions.

2. Instrumentation and methods

2.1 *Ground-based lidar measurements*

The National Astrophysical Observatory (NAO) of Georgia is located in the Abastumani (41° 45′ N, 42° 49′ E) mountainous region at approximately 1600 m above sea level (asl), some 100 km from the Black Sea. The NAO is equipped with a single-wavelength lidar system, which was designed to perform continuous measurements of suspended aerosol particles in the planetary boundary layer (PBL) and the lower free troposphere (LFT). It is based on a pulsed Nd:YAG (neodymium: yttrium aluminium garnet) laser source that emits at 1574 nm and has energy 70 mJ pulse^{-1}. The laser pulse duration is 10 ns and the repetition rate is 30 Hz. To retrieve the aerosol backscatter coefficient (β_{aer}), the standard Klett technique was applied (Klett 1985), which results in an average uncertainty on the retrieved value of β_{aer} of the order of 20–30%.

2.2 *Ground-based sunphotometric measurements*

To provide the aerosol optical and microphysical properties of the total atmospheric column, systematic sun photometric observations were performed by the well-known CIMEL radiometer (Cimel Electronique, Paris, France) (http://www.cimel.fr/index_us.html), which is a part of NASA's Aerosol Robotic Network (AERONET) (http://aeronet.gsfc.nasa.gov) (Holben *et al.* 2001). Since no CIMEL photometer was available in the study area, we used the one closest to the Abastumani instrument,

which is located at the Institute of Marine Sciences, Middle East Technical University, Erdemli, Turkey (36° 36′ N, 34° 18′ E, 3 m asl), on the southwestern coast of Turkey. According to Holben *et al.* (2001), the accuracy of the presented level 1.5 AOD measurements is of the order of ±0.03 (cloud-screened data). The sun photometer measures the solar radiance at 340, 380, 440, 500, 675, 870, 940 and 1020 nm wavelengths. Sky radiance (almucantar) measurements are done at 440, 675, 870 and 1020 nm. The data were used to retrieve the AOD, the aerosol single scattering albedo (SSA), the particle volume size distribution from 0.05 to 15 μm in particle radius and the complex refractive index in the range 1.33–1.60 (real part) and 0.0005i–0.5i (imaginary part) (Dubovik and King 2000).

2.3 *Space-borne lidar observations*

Space-borne active remote sensing of atmospheric aerosols and clouds is the key for providing global vertically resolved observations that are needed to better understand a variety of aerosol–cloud radiation climate feedback processes. The Cloud-Aerosol Lidar with Orthogonal Polarization (CALIOP) onboard CALIPSO has been providing information on the vertical distribution of aerosols and clouds as well as on their optical properties over the globe with unprecedented spatial resolution since June 2006 (Winker *et al.* 2007, 2009). CALIOP level 1 (version 3.01) data products were used in this study.

2.4 *Satellite AOD observations*

The Moderate Resolution Imaging Spectroradiometer (MODIS) was launched in December 1999 on the polar-orbiting Terra spacecraft, and since February 2000 has been acquiring daily global data in 36 spectral bands from the visible to the thermal infrared (29 spectral bands with 1 km, 5 spectral bands with 500 m and 2 spectral bands with 250 m, nadir pixel dimensions). The MODIS aerosol products are only created for cloud-free regions. The AOD values were retrieved by MODIS at 550 nm for both the ocean (best) and land (corrected) as described by the MODIS sensor website (http://modis-atmos.gsfc.nasa.gov/products.html). The MODIS Terra-derived AOD product over land (daily Level 2 aerosol products, i.e. MOD04 from Collection 5) at 10 km spatial resolution was acquired from the NASA Earth Observing System (EOS) Clearinghouse (ECHO). The expected errors in MODIS-derived AODs over land are $\pm(0.05 + 0.15 \times (\mathrm{AOD}))$ (Remer 2005, Remer *et al.* 2008). The error description and instrument validation are discussed by Engel-Cox *et al.* (2004) and by Chu *et al.* (2002) and Prasad and Singh (2009), respectively. Further details of the development of the aerosol retrieval algorithm over land are discussed by Remer *et al.* (2006).

2.5 *Dust modelling*

The updated version of the dust regional atmospheric model (BSC-DREAM8b) (Nickovic *et al.* 2001, Pérez *et al.* 2006a,b, Jiménez-Guerrero *et al.* 2008) has been delivering operational dust forecasts over the North Africa–Mediterranean–Middle East and Asian regions during the past years at the Barcelona Supercomputing Centre (BSC) (currently at www.bsc.es/projects/earthscience/DREAM/). The model simulates or predicts the three-dimensional field of the dust concentration in the troposphere. The dust model takes into account all major processes of the dust life cycle,

such as dust production, horizontal and vertical diffusion and advection and wet and dry deposition. The model also includes the effects of the particle size distribution on aerosol dispersion. The model numerically solves the Euler-type mass partial differential equation by integrating it spatially and temporally. The dust production is parameterized using near-surface turbulence and stability, as well as soil features. The dust production mechanism is based on viscous/turbulent mixing close to the surface and soil moisture content. In BSC-DREAM8b, the aerosol description is improved from 4 to 8 bins and dust radiation interactions are included. For this study, BSC-DREAM8b simulation is initialized with 24-hourly (at 00:00 UTC) updated NCEP (National Centers for Environmental Prediction) $0.5^\circ \times 0.5^\circ$ analysis data and the initial state of the dust concentration in the model is defined by the 24-hour forecast from the previous-day model run because there are not yet satisfactory three-dimensional dust concentration observations to be assimilated. The resolution is set to $1/3^\circ$ ($\sim$50 km) in the horizontal and to 24 layers extending up to approximately 15 km in the vertical.

3. Results and discussion

During April and May 2009, the dust activity was very pronounced over the south-eastern Mediterranean and the southwestern Asian regions, as usually happens during the spring period in the northern hemisphere (Liu *et al.* 2008a). More specifically, for the time period from 1 to 5 May 2009, over southwestern Turkey at Erdemli (see map of figure 1, lower yellow circle), the AOD values observed were quite high (up to $\sim$0.57 at 340 nm) at all wavelengths of the CIMEL instrument (table 1).

According to table 1, we observed that for the period 1 to 5 May, the AOD values at 500 nm varied from small (0.12 under low aerosol load) to high (up to 0.51 under high aerosol load), with a mean value of 0.24 ± 0.09. In addition, the aerosol Ångström exponent (α) was found to vary from 0.16 to 0.92, indicating the large variability of the aerosol size distribution due to mixing of different types of aerosol particles and the dominance of rather coarse particles in the atmosphere. More specifically, the minimum value of the Ångström exponent reached the value of 0.158 on 4 May, whereas the mean daily value of α was of the order of 0.184. On the same day, the AOD values ranged from 0.35 to 0.55 in different wavelengths, whereas the mean daily AOD values at 500 nm were of the order of 0.45. The CIMEL measurements strongly indicate that 4 May was the day on which the dust was maximum over Erdemli, Turkey.

In figure 1, MODIS near real time (NRT) true colour images are presented for 4 May ((*a*), upper panel) and 5 May ((*b*), upper panel), showing the dust evolution over the study area. It is evident that dust is present over Abastumani on 5 May, and that the MODIS capture is contaminated by clouds. In figure 1, the MODIS Level 2, Collection 5 AODs at 550 nm with a 10 km $\times$ 10 km resolution obtained on 4 May ((*a*), lower panel) and 5 May ((*b*), lower panel) are presented. Although the presence of cloud does not allow AOD retrievals over the stations examined here, it is evident, especially for 5 May, that the AOD values near Abastumani reached values greater than 1. Examining the MODIS 50×50 km AOD retrievals at 550 nm (not shown here), we see that the AOD reached its highest value ($>$0.8) over Erdemli on 4 May, while it reached 0.9 over Abastumani on 5 May. These AOD values are typical under strong dust loadings (Holben *et al.* 2001, Papayannis *et al.* 2005, Liu *et al.* 2008b, Papayannis *et al.* 2008) near the dust source regions.

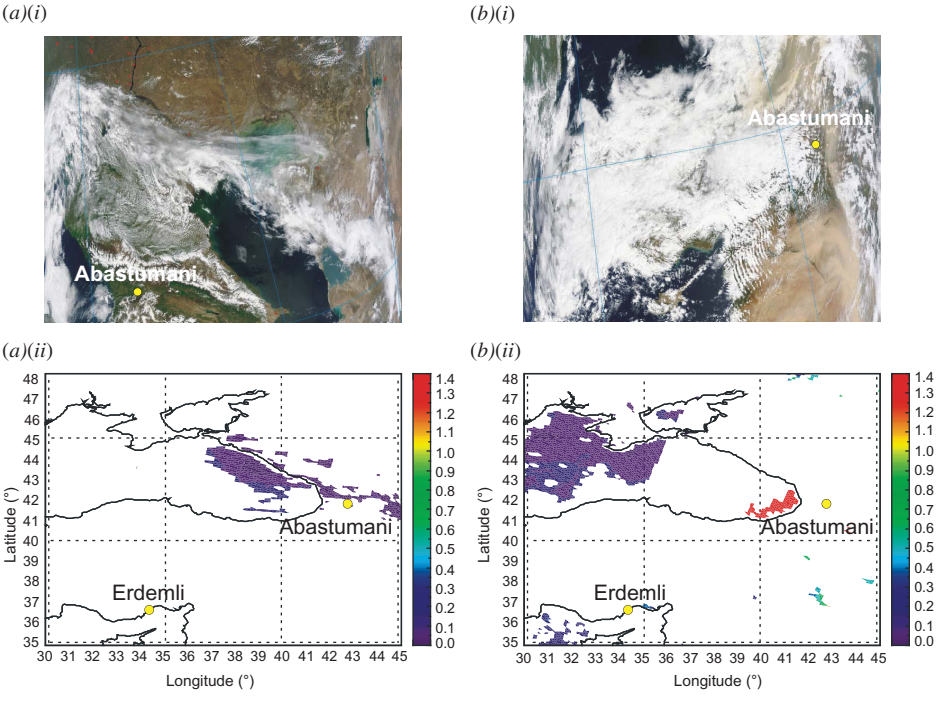

Figure 1. MODIS – Terra NRT (near real time) Level 2 true colour images (upper panels, (*a*)(*i*) and (*b*)(*i*)) and corresponding AOD at 550 nm (lower panels, (*a*)(*ii*) and (*b*)(*ii*)) (Level 2, Collection 5) at 10 km resolution on 4 May 2009 (*a*) and 5 May 2009 (*b*). The sites of Erdemli (Turkey) and Abastumani (Georgia) are denoted by the upper and lower yellow circles in the AOD maps, respectively.

Table 1. Mean, standard deviation of the mean (S_{dev}), maximum and minimum values of AOD and aerosol Ångström exponent (α), for the time period from 1 to 5 May 2009, as retrieved from CIMEL sun photometry at Erdemli, Turkey.

AOD at wavelength (nm)	Mean value	S_{dev} value	Max value	Min value
1020	0.136	0.079	0.451	0.060
870	0.153	0.081	0.467	0.075
675	0.179	0.083	0.481	0.085
500	0.244	0.092	0.509	0.115
440	0.273	0.099	0.519	0.125
380	0.318	0.108	0.538	0.144
340	0.355	0.114	0.566	0.156
α (440/870)	0.920	0.283	1.347	0.158

In figure 2, we present the temporal evolution of the mean aerosol particle radius (in μm) versus the volume size distribution (in $\mu m^3\ \mu m^{-2}$) during the studied period (1–5 May) over Erdemli. It is evident from this figure that during 1–2 May, a small number of particles with mean radius of 2–4.5 μm were present. On the following days (3–5 May), due to the prevailing southwestern winds, the volume size distribution of the aerosol particles started to increase, reaching its maximum value (around 0.18 $\mu m^3\ \mu m^{-2}$) on 4 May. Thus, in the studied period, we observed the dominance of

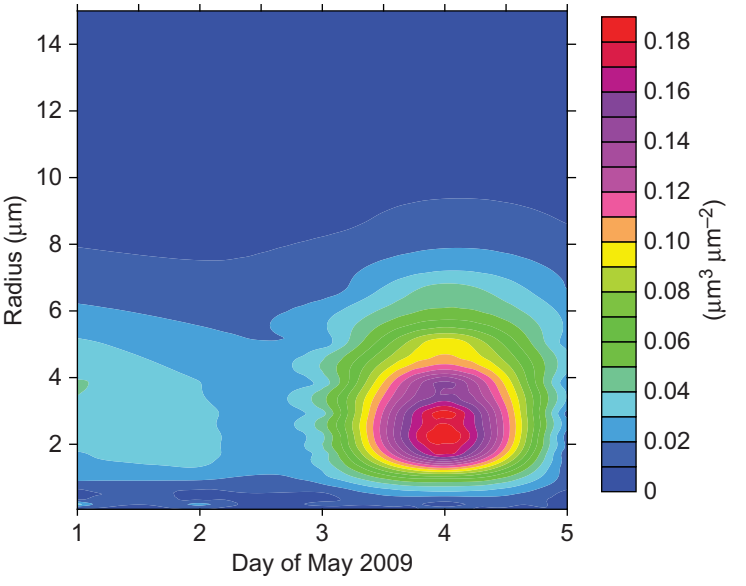

Figure 2. Time evolution of the mean aerosol radius (in μm) versus their volume size distribution over Erdemli (Turkey) from 1 to 5 May 2009.

rather coarse particles (with a radius of the order of 1–6 μm), with the maximum (almost more than double) value of the volume size aerosol distribution again present on 4 May. These coarse particles could be related to the transport of dust particles over the CIMEL site in Turkey during the previous days, as we will present in the following.

The transport of a strong dust load from the Saharan and the western Asian desert sources over Erdemli was simulated with the BSC-DREAM8b dust model for 4 and 5 May (figure 3 shows the results every 12 hours for the 20° W–70° E domain). According to this model, the dust load varied from 0.50 to 0.75 g m^{-2} south of Cyprus and from 0.25 to 0.75 g m^{-2} over Erdemli (4 May, 00:00 UTC). Twelve hours later (4 May, 12:00 UTC), the dust load varied from 0.75 to 1.5–2.5 g m^{-2} over Erdemli and from 0.05 to 0.25 g m^{-2} over Abastumani. The following day (5 May, 00:00 UTC), the dust load varied from 0.05 to 0.25 g m^{-2} over Abastumani and Erdemli. The same situation occurred over Abastumani on 5 May (12:00 UTC), where the dust load varied from 0.25 to 0.50 g m^{-2}. On the other hand, over Erdemli, the dust had been completely advected to southeastern directions. The following day (6 May, 00:00 UTC), the dust load moved more eastwards and the aerosol dust load was again reduced (not shown here). Thus, from the BSC-DREAM8b model and because of the specific meteorological conditions prevailing over the eastern Mediterranean region, the dust plume first arrived over Cyprus, then moved over Erdemli and later shifted northeastwards over Abastumani on 4 May, and reached its maximum intensity there on 5 May. Almost overcast conditions prevailing over Georgia on 4 May did not permit lidar measurements onsite during that day. However, on 5 May, clear sky with scattered clouds did permit the aerosol lidar system of NAO to perform measurements and thus to detect the dust layer arriving over Abastumani.

The daily composite of the vertical profiles (altitude in metres, above mean sea level) of the range-corrected backscattered lidar signal (RCS) in arbitrary units (AU) is presented in figure 4, from 08:50 to 10:06 UTC on 5 May. From this figure, it is

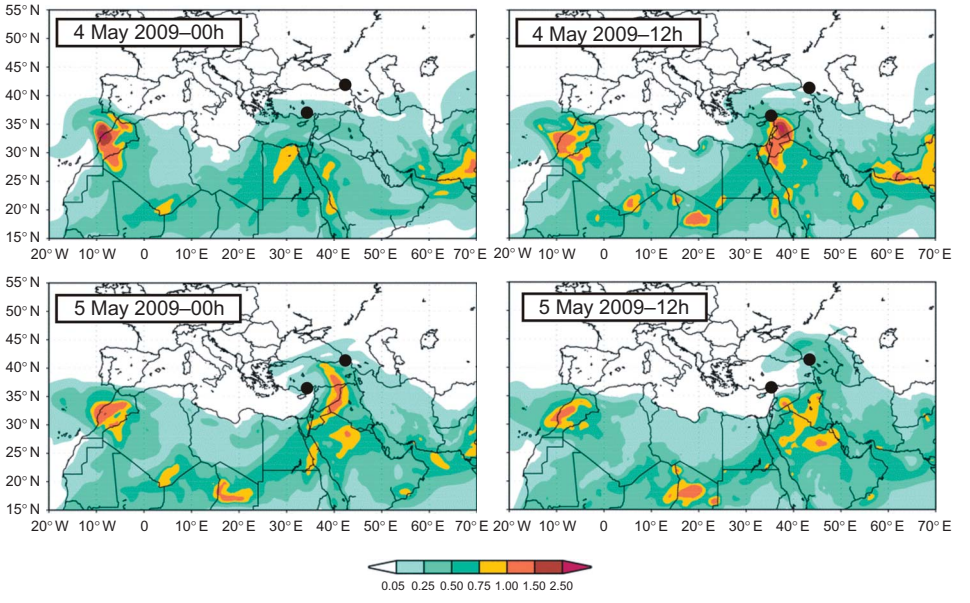

Figure 3. Temporal evolution (every 12 hours) of the dust load concentration (g m^{-2}) around the Mediterranean area as predicted from the BSC-DREAM8b model during the pick of the dust event (4 and 5 May). Erdemli (Turkey) and Abastumani (Georgia) are denoted by the black circles.

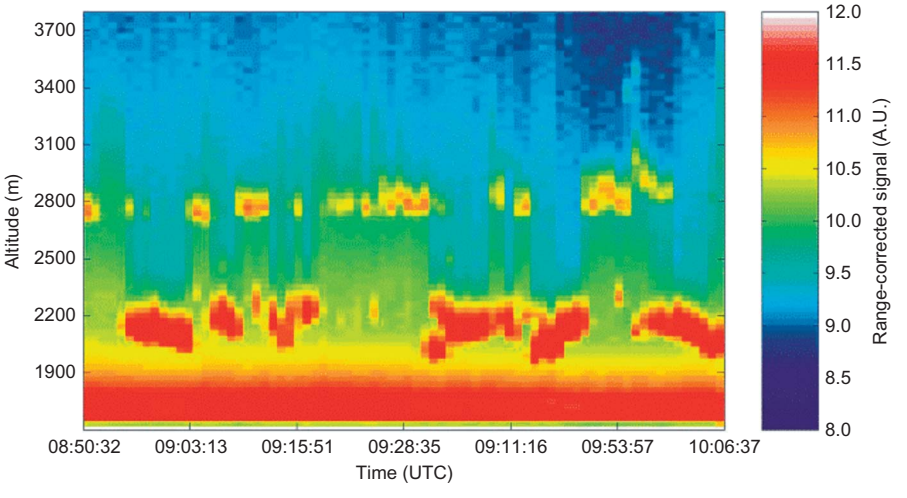

Figure 4. The temporal evolution of the range-corrected signal (in arbitrary units, AU) versus altitude (m) above mean sea level (asl) over Abastumani (Georgia) on 5 May 2009 (08:50–10:06 UTC).

obvious that the dust particles reached Abastumani at different heights, from 2100 up to around 3400 m asl, but they were also present at even lower heights inside the PBL located that day around 2100 m. Aerosol particle growth due to high relative humidity and subsequent cloud formation could explain the presence of low-altitude clouds just

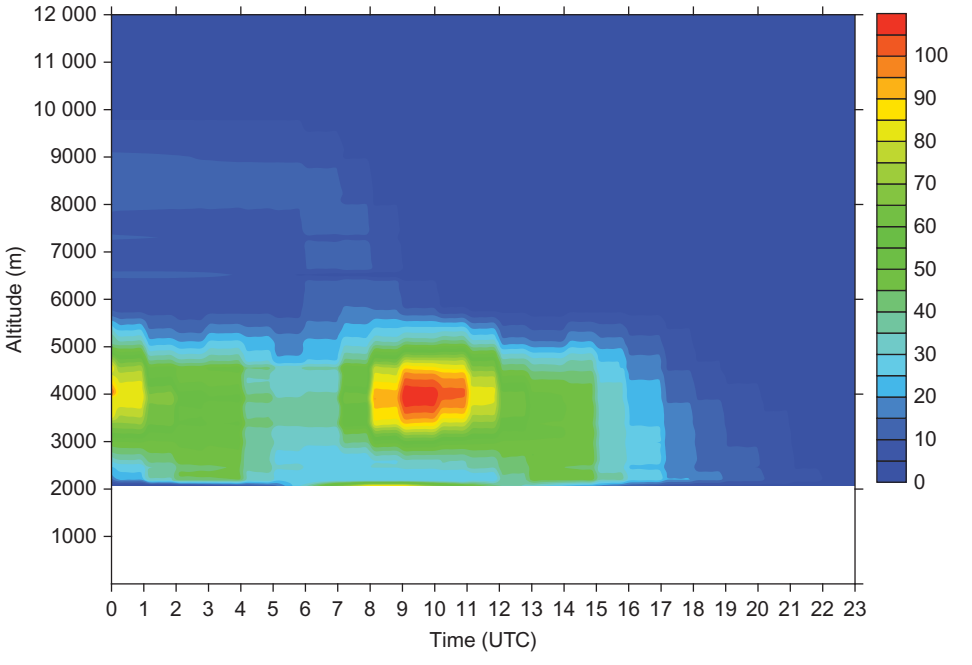

Figure 5. The temporal evolution of the dust concentration profile ($\mu g\ m^{-3}$) versus altitude (m) above mean sea level (asl) over Abastumani (Georgia) on 5 May 2009, as predicted by the BSC-DREAM8b dust model.

above the PBL (around 2150 and 2800 m). The presence of strong low clouds around 2150 m prevents, for certain short time periods, the full propagation of the laser pulse in the lower troposphere and thus no lidar data can be obtained further than 3700 m height.

In figure 5, we present the temporal evolution of the dust concentration profile (in $\mu g\ m^{-3}$) (Georgia) on 5 May 2009, as predicted by the BSC-DREAM8b dust model. The dust vertical distribution is simulated for every hour at heights from 2 up to 12 km asl. We can see that for that day, a strong dust layer was forecast between heights of 2 and 5 km, mostly between 08:00 UTC and 12:00 UTC, while a less strong dust layer was forecast at the same heights between 00:00 and 04:00 UTC. The dust layers started to descend and dissipate around 16:00 UTC. Comparing figures 4 and 5 for the period between 08:50 and 10:06 UTC, we can see that in the height range 2000–3400 m asl, the BSC-DREAM8b dust model is able to reproduce, quite correctly, the aerosol dust layers observed by the NAO lidar over Abastumani.

To verify the origin of the air masses arriving over Abastumani at heights 2.1, 2.7 and 3.4 km asl on 5 May at 09:00 UTC, we used the HYSPLIT model (Draxler and Rolph 2003) in the backward mode (figure 6). From this figure, it is obvious that all air masses arriving between heights of 2.7 and 3.4 km over Abastumani originated from the northern Saharan dust region, whereas those that arrived at 2.1 km originated from the Arabian desert. The latter ones are probably enriched even more with dust particles, since they had passed over desert soils at ground level (some 24–72 hours before) before rising to 2.1 km.

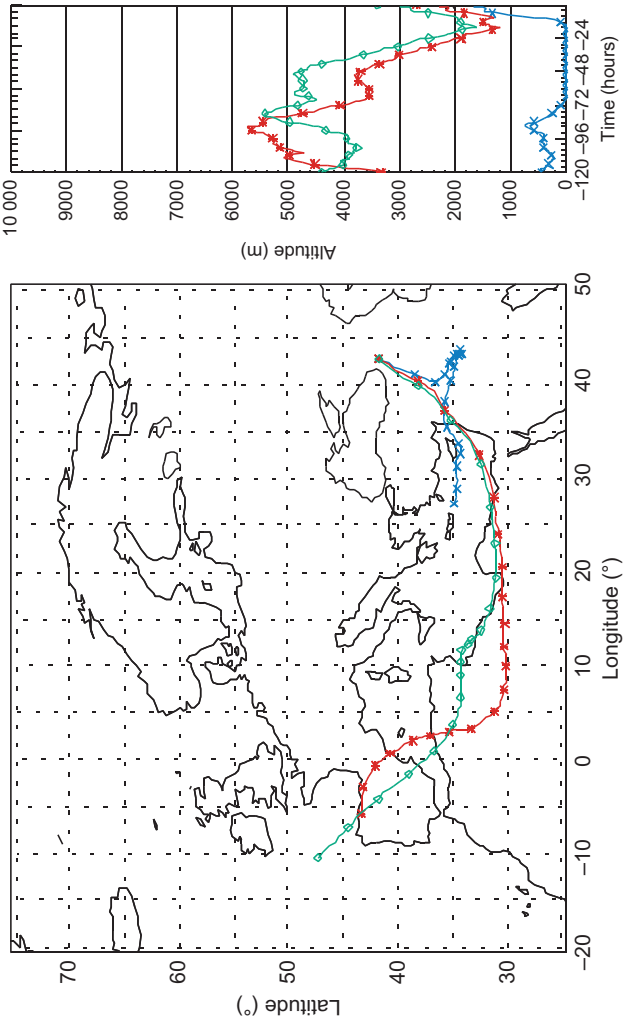

Figure 6. Backward air mass trajectories arriving over Abastumani (Georgia) on 5 May 2009 (09:00 UTC) at various height levels (2.1, 2.7 and 3.4 km asl).

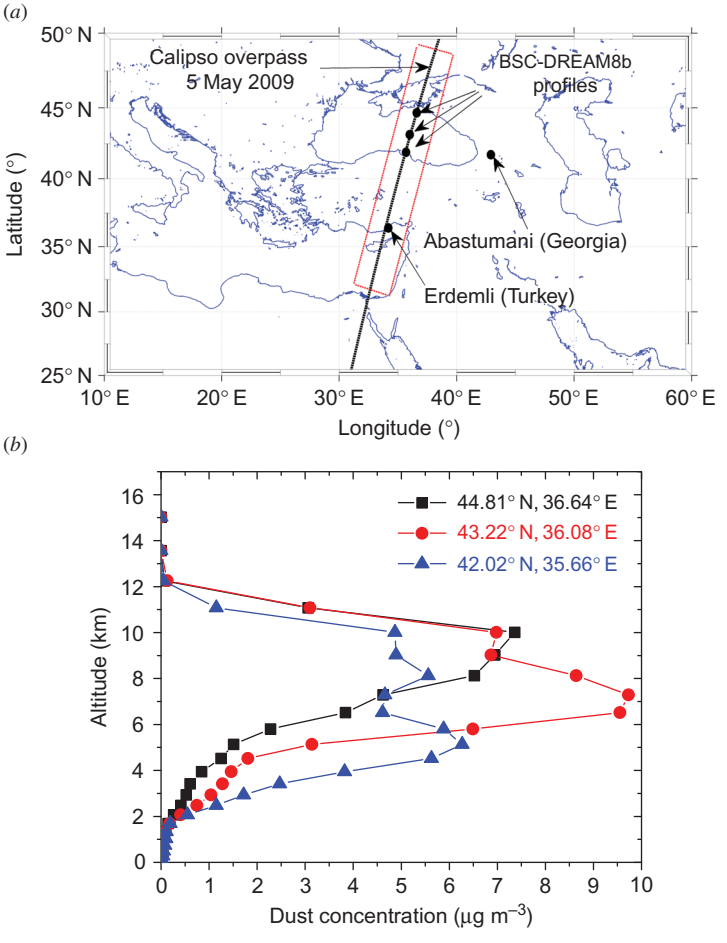

Figure 7. (*a*) CALIPSO lidar ground track for 5 May 2009 (23:55 UTC) from 24.9° N, 30.5° E to 50° N, 38° E. The Erdemli and the Abastumani areas are also indicated. (*b*) Vertical profiles of the aerosol dust concentration (μg m^{-3}) for three sites over the Black Sea (42.02° N, 35.66° E to 44.81° N, 36.64° E), as predicted by the BSC-DREAM8b model.

To corroborate our ground observations obtained over Abastumani, we used the CALIOP lidar measurements performed onboard the CALISPO satellite (Winker *et al.* 2007, 2009). The CALIOP ground track passes 500 km west of Abastumani and only a few kilometres west of Erdemli (figure 7(*a*)). Therefore, we selected three collocated sites (44.81° N, 36.64° E; 43.22° N, 36.08° E; 42.02° N, 35.66° E) over the Black Sea along the CALIOP ground track, which were closer to the Abastumani site, where we ran the BSC-DREAM8b dust model. The corresponding vertical profiles of the dust concentration are given in figure 7(*b*). From figure 7(*b*), we see that the dust is concentrated at heights from 2 to 12 km asl, with a centre of mass (Papayannis *et al.* 2008) of the order of 9 km (44.81° N, 36.64° E), 8 km (43.22° N, 36.08° E) and 7 km (42.02° N, 35.66° E), respectively. More specifically, at 44.81° N, 36.64° E, BSC-DREAM8b simulated an intense 5 km-thick dust layer that peaked at 10 km asl (7 μg m^{-3}). Dust presence was also simulated at heights from 2 up to 6 km.

At 43.22° N, 36.08° E, BSC-DREAM8b predicts a more intense 7–8 km thick dust layer that peaks at 7.5 km asl (10 $\mu g\ m^{-3}$). Finally, at 42.02° N, 35.66° E, BSC-DREAM8b simulates a less intense 8-km thick dust layer that peaks between 5 and 8 km asl (5–6 $\mu g\ m^{-3}$).

Figure 8(*a*) shows that CALIOP observations (data level 3.0.1) obtained on 5 May (around 23:55 UTC) in terms of the total attenuated backscatter at 532 nm confirm the presence of a high aerosol load over Turkey and Georgia from ground up to even a height of 10 km in the region from 49.42° N, 38.40° E to 32° N, 33° E. More specifically, this figure shows the presence of strong dust layers at heights between 8 and 10 km (around 49° N, 38° E) and between 7 and 9 km (around 42° N, 35° E), whereas less strong dust layers were visible at heights between ground and 3–3.5 km between 44.81° N, 36.64° E and 42.02° N, 35.66° E (over the Black Sea) and around 31.5° N, 33° E (south of Cyprus). These dust layers are denoted by the yellow colour pixels (figure 8(*a*)) and show low depolarization (<0.2) (figure 8(*b*)). Moreover, they are much more discernable in figures 8(*c*) and (*d*), where the CALIPSO data analysis algorithms provide the regions where dust or clouds are present (figure 8(*c*) – clouds are given by the light blue colour pixels and aerosols are given by the orange colour code pixels; figure 8(*d*) – dust is given by the yellow or brown colour pixels).

In figure 8(*c*), the vertical feature mask (version 3.01) during the CALIPSO overpass over Cyprus–Turkey–Black Sea–southern Russia on 5 May 2009, from ground up to a height of 11 km is presented. The CALIOP data denote the presence of clouds (light blue pixels) mixed with aerosols from 3.5 km down to ground when passing from 44.81° N, 36.64° E to 42.02° N, 35.66° E (over the Black Sea). As discussed previously, when passing from 49.46° N, 38.42° E to 37.40° N, 34.23° E, CALIPSO detects strong aerosol layers at heights between 7 and 10 km, mixed with clouds at the same heights or downsloping from 5 to 2 km asl (light blue colour pixels). This correlates very well with the mixing of clouds and dust observed by the NAO lidar over Abastumani (figure 4).

Thus, over the Black Sea (between the red vertical lines), the CALIOP data confirm the presence of dust layers both from ground up to heights of 3–3.5 km and between 7 and 9 km, which were in accordance with those forecast by the BSC-DREAM8b model, already shown in figures 3 and 7. Moreover, the CALIOP data (figure 8(*d*)) do confirm, as well, the transport of dust from the Saharan region (28° N, 31.5° E) up to the Black Sea (43° N, 36° E) and even up to southern Russia (50° N, 38.5° E). Most of the times, CALIOP shows the mixing of dust aerosols with clouds, as also seen by the RCS data over Abastumani.

At this point, we have to mention that BSC-DREAM8b predicted quite successfully mostly the peak of the dust layers (figure 7(*b*)) at three locations over the Black Sea (mostly at heights between 5 and 10 km); thus, the correlation between the model and CALIPSO dust data is quite good. On the contrary, in the altitude range of height 4–7 km, between 44.81° N, 36.64° E and 42.02° N, 35.66° E, the correlation between the model and CALIPSO dust data is quite bad, since CALIPSO detects mostly clean air and few clouds mixed with dust, whereas the model forecast always the presence of strong dust layers. This disagreement over the region 43.22° N, 36.08° E and 42.02° N, 35.66° E could be related to the fact that CALISPO, under specific conditions, performs erroneous cloud and aerosol classification when version 2.02 CALIOP data are used (Liu *et al.* 2004, Kim *et al.* 2008, Chen *et al.* 2010). However, our NAO RCS lidar data do confirm the existence of mixing of dust and clouds over Abastumani, thus

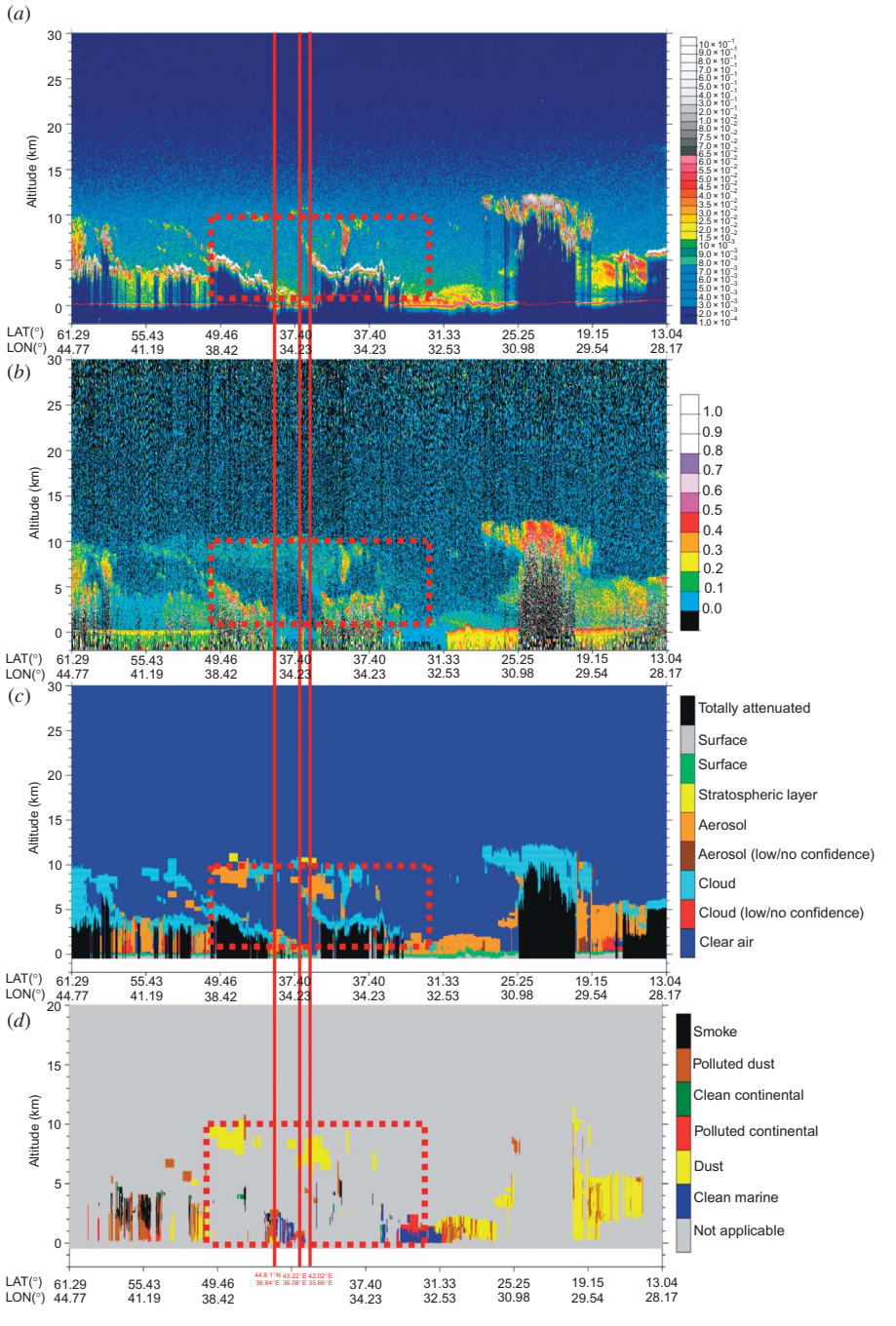

Figure 8. Calipso vertical profiles of the (*a*) total attenuated backscatter (532 nm, km^{-1} sr^{-1}), (*b*) depolarization ratio, (*c*) vertical feature mask and (*d*) aerosol type along the CALIPSO ground track from 61.29° N, 44.77° E to 13.04° N, 28.17° E.

validating the CALIOP level 3.01 data obtained at the nearby location of the Black Sea (500 km apart) and used in this article. However, the discrimination between dust and clouds has to be further investigated when the newly released level 3.01 CALIOP data are used in conjunction with co-located ground-based lidar data.

4. Summary and conclusions

In this article, we presented aerosol optical properties and vertical layering during a strong dust event, as followed by a CIMEL sun photometer located at Erdemli (Turkey) and by an aerosol lidar system situated at Abastumani (Georgia). We found that the high aerosol load forecast by the BSC-DREAM8b model was confirmed by CIMEL data on 4 May over Turkey, where the corresponding maximum value of the aerosol volume size distribution was of the order of 0.18 μm^3 μm^{-2}, with a mean aerosol radius of 2 μm. Aerosol observations during dust outbreaks obtained from MODIS showed that the AOD values at 550 nm were of the order of 0.9 over Georgia, whereas the AOD values from the CIMEL over Turkey ranged between 0.3 and 0.6. The corresponding Angström exponent (α) values were of the order of 0.50–0.65, while the mean value of α was smaller than 1, indicating the dominance of large aerosols over the area. The coarse particle contribution to the total AOD was estimated approximately to be 57%. The presence of the dust layer was detected on 5 May both by a ground-based lidar over Abastumani and by the CALIOP lidar onboard the CALISPO satellite along its orbit over Georgia, for the first time to our knowledge in that area. The dust layer seemed to extend from near ground up to 11.5 km, with a horizontal distance of approximately 5500 km. The profiles of dust load volume concentration, concerning locations on CALIPSO overpasses, provided by BSC-DREAM8b, showed good correlation only concerning the peak altitudes. The discrimination between dust and clouds seems to be further clarified when version 3.01 CALIOP data were used, in contrast to the erroneous cloud and aerosol classification when level 2.01 data were used.

Acknowledgements

CALIPSO data were obtained from the NASA Langley Research Center Atmospheric Science Data Center. The authors also thank the CALIPSO team of the NASA Langley Research Center for the provision of the CALIPSO ground track data. The atmospheric meteorological products were provided by the NOAA through the Real-time Environmental Applications and Display system. The CIMEL data were provided by the AERONET network station located at the IMS-METU-ERDEMLI (Turkey). Analyses and visualizations of the MODIS data used in this article were produced with the Giovanni Online Data System, developed and maintained by the NASA GES DISC. The editor and the reviewers of this article are gratefully acknowledged for their comments and corrections.

References

Chen, B., Huang, J., Minnis, P., Hu, Y., Yi, Y., Liu, Z., Zhang, D. and Wang, X., 2010, Detection of dust aerosol by combining CALIPSO active lidar and passive IIR measurements. *Atmospheric Chemistry and Physics*, **10**, pp. 4241–4251.

Chu, D.A., Kaufman, Y.J., Ichoku, C., Remer, L.A., Tanré, D. and Holben, B.N., 2002, Validation of MODIS aerosol optical depth retrieval over land. *Geophysical Research Letters*, **29**, p. 8007.

Draxler, R.R. and Rolph, G.D., 2003, HYSPLIT (HYbrid Single-Particle Lagrangian Integrated Trajectory) model access via NOAA ARL READY website. NOAA Air Resources Laboratory, Silver Spring, MD. Available online at: http://www.arl.noaa.gov/ready/hysplit4.html

Dubovik, O. and King, M.D., 2000, A flexible inversion algorithm for retrieval of aerosol optical properties from sun and sky radiance measurements. *Journal of Geophysical Research*, **105**, pp. 20673–20696.

Engel-Cox, J.A., Holloman, C.H., Coutant, B.W. and Hoff, R.M., 2004, Qualitative and quantitative evaluation of MODIS satellite sensor data for regional and urban scale air quality. *Atmospheric Environment*, **38**, pp. 2495–2509.

Engelstaedter, S. and Washington, R., 2007, Temporal controls on global dust emissions: the role of surface gustiness. *Geophysical Research Letters*, **34**, L15805, doi:10.1029/2007GL029971.

Escudero, M., Querol, X., Ávila, A. and Cuevas, E., 2007a, Origin of the exceedances of the European daily PM limit value in regional background areas of Spain. *Atmospheric Environment*, **41**, pp. 730–744.

Escudero, M., Querol, X., Pey, J., Alastuey, A., Pérez, N., Ferreira, F., Cuevas, E., Rodriguez, S. and Alonso, S., 2007b, A methodology for the quantification of the net African dust load in air quality monitoring networks. *Atmospheric Environment*, **41**, pp. 5516–5524.

Forster, P., Ramaswamy, V., Artaxo, P., Berntsen, T., Betts, R., Fahey, D.W., Haywood, J., Lean, J., Lowe, D.C., Myhre, G., Nganga, J., Prinn, R., Raga, G., Schulz, M. and Van Dorland, R., 2007, Changes in atmospheric constituents and in radiative forcing. In *Climate Change 2007: The Physical Science Basis. Contribution of Working Group I to the Fourth Assessment Report of the Intergovernmental Panel on Climate Change*, S. Solomon, D. Qin, M. Manning, Z. Chen, M. Marquis, K.B. Averyt, M. Tignor and H.L. Miller (Eds.) (Cambridge, UK: Cambridge University Press) pp. 129–234.

Holben, B.N., Tanré, D., Smirnov, A., Eck, T.F., Slutsker, I., Abuhassan, N., Newcomb, W.W., Schafer, J.S., Markham, B., Frouin, D.C.R., Halthore, R., KarnelI, A., O'neill, N.T., Pietras, C., Pinker, R.T., Voss, K. and Zibordi, G., 2001, Aerosol optical depth from AERONET. *Journal of Geophysical Research*, **106**, pp. 12067–12098.

Jiménez-Guerrero, P., Pérez, C., Jobra, O. and Baldasano, J., 2008, Contribution of Saharan dust in an integrated air quality system and its on-line assessment. *Geophysical Research Letters*, **35**, L03814, doi:10.1029/2007GL031580.

Kim, S.-W., Berthier, S., Raut, J.-C., Chazette, P., Dulac, F. and Yoon, S.-C., 2008, Validation of aerosol and cloud layer structures from the space-borne lidar CALIOP using a ground-based lidar in Seoul, Korea. *Atmospheric Chemistry and Physics*, **8**, pp. 3705–3720.

Kinne, S., Schulz, M., Textor, C., Guibert, S., Balkanski, Y., Bauer, S.E., Berntsen, T., Berglen, T.F., Boucher, O., Chin, M., Collins, W., Dentener, F., Diehl, T., Easter, R., Feichter, J., Fillmore, D., Ghan, S., Ginoux, P., Gong, S., Grini, A., Hendricks, J., Herzog, M., Horowitz, L., Isaksen, I., Iversen, T., Kirkevåg, A., Kloster, S., Koch, D., Kristjansson, J.E., Krol, M., Lauer, A., Lamarque, J.F., Lesins, G., Liu, X., Lohmann, U., Montanaro, V., Myre, G., Penner, J., Pitari, G., Reddy, S., Seland, O., Stier, P., Takemura, T. and Tie, X., 2006, An AeroCom initial assessment – optical properties in aerosol component modules of global models. *Atmospheric Chemistry and Physics*, **6**, pp. 1815–1834.

Klett, J.D., 1985, Lidar inversion with variable backscatter/extinction ratios. *Applied Optics*, **24**, pp. 1638–1643.

Liu, D., Wang, Z., Liu, Z., Winker, D. and Trepte, C., 2008a, A height resolved global view of dust aerosols from the first year CALIPSO lidar measurements. *Journal of Geophysical Research*, **113**, D16214, doi:10.1029/2007JD009776.

Liu, Z., Liu, D., Huang, J., Vaughan, M., Uno, I., Sugimoto, N., Kittaka, C., Trepte, C., Wang, Z., Hostetler, C. and Winker, D., 2008b, Airborne dust distributions over the Tibetan Plateau and surrounding areas derived from the first year of CALIPSO lidar observations. *Atmospheric Chemistry and Physics*, **8**, pp. 5045–5060.

Liu, Z., Vaughan, M.A., Winker, D.M., Hostetler, C.A., Poole, L.R., Hlavka, D., Hart, W. and McGill, M., 2004, Use of probability distribution functions for discriminating between cloud and aerosol in lidar backscatter data. *Journal of Geophysical Research*, **109**, D15202, doi:10.1029/2004JD004732.

Marticorena, B., Bergametti, G., Aumont, B., Callot, Y., N'Doumé, C. and Legrand, M., 1997, Modeling the atmospheric dust cycle: 2. Simulation of Saharan dust sources. *Journal of Geophysical Research*, **102**, pp. 4387–4404.

Nickovic, S., Kallos, G., Papadopoulos, A. and Kakaliagou, O., 2001, A model for prediction of desert dust cycle in the atmosphere. *Journal of Geophysical Research*, **106**, pp. 18113–18129.

Papayannis, A., Amiridis, V., Mona, L., Tsaknakis, G., Balis, D., Bösenberg, J., Chaikovski, A., De Tomasi, F., Grigorov, I., Mattis, I., Mitev, V., Müller, D., Nickovic, S., Pérez, C., Pietruczuk, A., Pisani, G., Ravetta, F., Rizi, V., Sicard, M., Trickl, T., Wiegner, M., Gerding, M., Mamouri, R.E., D'amico, G. and Pappalardo, G., 2008, Systematic lidar observations of Saharan dust over Europe in the frame of EARLINET (2000–2002). *Journal of Geophysical Research*, **113**, D10204, doi: 10.1029/2007JD009028.

Papayannis, A., Balis, D., Amiridis, V., Chourdakis, G., Tsaknakis, G., Zerefos, C., Castanho, A.D.A., Nickovic, S., Kazadzis, S. and Grabowski, J., 2005, Measurements of Saharan dust aerosol over Eastern Mediterranean using elastic backscatter-Raman lidar, spectrophotometric and satellite observations in the frame of the EARLINET project. *Atmospheric Chemistry and Physics*, **5**, pp. 2065–2079.

Pérez, C., Nickovic, S., Baldasano, J.M., Sicard, M., Rocadenbosch, F. and Cachorro, V.E., 2006a, A long Saharan dust event over the western Mediterranean: lidar, sun photometer observations, and regional dust modelling. *Journal of Geophysical Research*, **111**, D15214, doi:10.1029/2005JD006579.

Pérez, C., Nickovic, S., Pejanovic, G., Baldasano, J.M. and Ozsoy, E., 2006b, Interactive dust-radiation modeling: a step to improve weather forecasts. *Journal of Geophysical Research*, **111**, D16206, doi:10.1029/2005JD006717.

Prasad, A.K. and Singh, R.P., 2009, Validation of MODIS Terra, AIRS, NCEP/DOE AMIP-II Reanalysis-2, and AERONET sun photometer derived integrated precipitable water vapor using ground-based GPS receivers over India. *Journal of Geophysical Research*, **114**, D05107, doi:10.1029/2008JD011230.

Prospero, J.M., Ginoux, P., Torres, O., Nicholson, S.E. and Gill, T., 2002, Environmental characterization of global sources of atmospheric soil dust identified with Nimbus 7 Total Ozone Mapping Spectrometer (TOMS) absorbing aerosol product. *Review of Geophysics*, **40**, p. 1002.

Querol, X., Alastuey, A., Pey, J., Cusack, M., Pérez, N., Mihalopoulos, N., Theodosi, C., Gerasopoulos, E., Kubilay, N. and Koçak, M., 2009a, Variability in regional background aerosols within the Mediterranean. *Atmospheric Chemistry and Physics*, **9**, pp. 4575–4591.

Querol, X., Pey, J., Pandolfi, M., Alastuey, A., Cusack, M., Pérez, N., Moreno, T., Viana, M., Mihalopoulos, N., Kallos, G. and Kleanthous, S., 2009b, African dust contributions to mean ambient PM_{10} mass-levels across the Mediterranean Basin. *Atmospheric Environment*, **43**, pp. 4266–4277.

Ramanathan, V., Ramana, M., Roberts, G., Kim, D., Corrigan, C., Chung, C. and Winker, D., 2007, Warming trends in Asia amplified by brown cloud solar absorption. *Nature*, **448**, pp. 575–578.

Remer, L.A., 2005, The MODIS aerosol algorithm, products and validation. *Journal of Atmospheric Science*, **62**, pp. 947–973.

Remer, L.A., Kleidman, R.G., Levy, R.C., Kaufman, Y.J., Tanré, D., Mattoo, S., Martins, J.V., Ichoku, C., Koren, I., Yu, H. and Holben, B.N., 2008, Global aerosol climatology from the MODIS satellite sensors. *Journal of Geophysical Research*, **113**, D14S07, doi:10.1029/2007JD009661.

Remer, L.A., Tanré, D., Kaufman, Y.J., Levy, R. and Mattoo, S., 2006, Algorithm for remote sensing of tropospheric aerosols from MODIS, Collection 5, Product ID: MOD04/MYD04. Available online at: http://modis.gsfc.nasa.gov/data/atbd/atbd_mod02.pdf (accessed 11 January 2006).

Rodriguez, S., Querol, X., Alastuey, A., Kallos, G. and Kakaliagou, O., 2001, Saharan dust contributions to PM_{10} and TSP levels in Southern and Eastern Spain. *Atmospheric Environment*, **35**, pp. 2433–2447.

Tegen, I., Lacis, A.A. and Fung, I., 1996, The influence on climate forcing of mineral aerosols from disturbed soils. *Nature*, **380**, pp. 419–422.

Winker, D.M., Hunt, W.H. and McGill, M.J., 2007, Initial performance assessment of CALIOP. *Geophysical Research Letters*, **34**, L19803, doi:10.1029/2007GL030135.

Winker, D.M., Vaughan, M., Omar, A., Hu, Y., Powell, K.A., Liu, Z., Hunt, W.H. and Young, S.A., 2009, Overview of the CALIPSO mission and CALIOP data processing algorithms. *Journal of Atmospheric and Oceanic Technology*, **26**, pp. 2310–2323.